



The 9th Asian Triangle Heavy-Ion Conference

Application of the Momentum Kick Model with multiplicity dependence to the pp collisions at $\sqrt{s} = 13$ TeV

Jeongseok Yoon with Prof. Jin-Hee Yoon

Department of Physics, Inha University, Incheon, Republic of Korea

Apr 26. 2023

Motivation

Ridge structure

- Two-particle(trigger and associated particles) correlation phenomenon.
- Similar to “mountain ridge.”
- Provide insight into particle production.

Heavy-Ion collisions
(such as PbPb and AuAu collisions)

Explained well by QGP
(hydrodynamic models)

Small systems & High-multiplicity
(such as pp and p-Pb collisions)

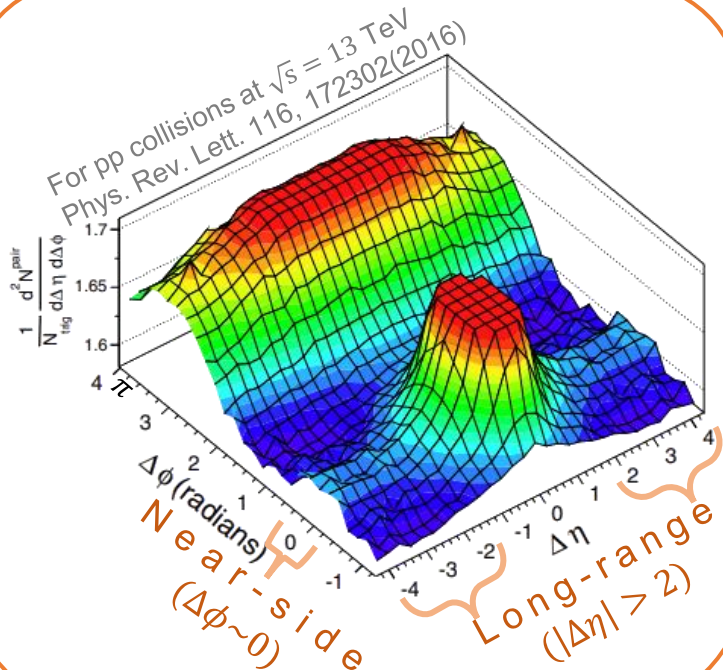
Insufficient density and temperature in small systems.

Limitation

Therefore, the hydrodynamic models are still **controversial**.

∴ Momentum Kick Model (MKM)

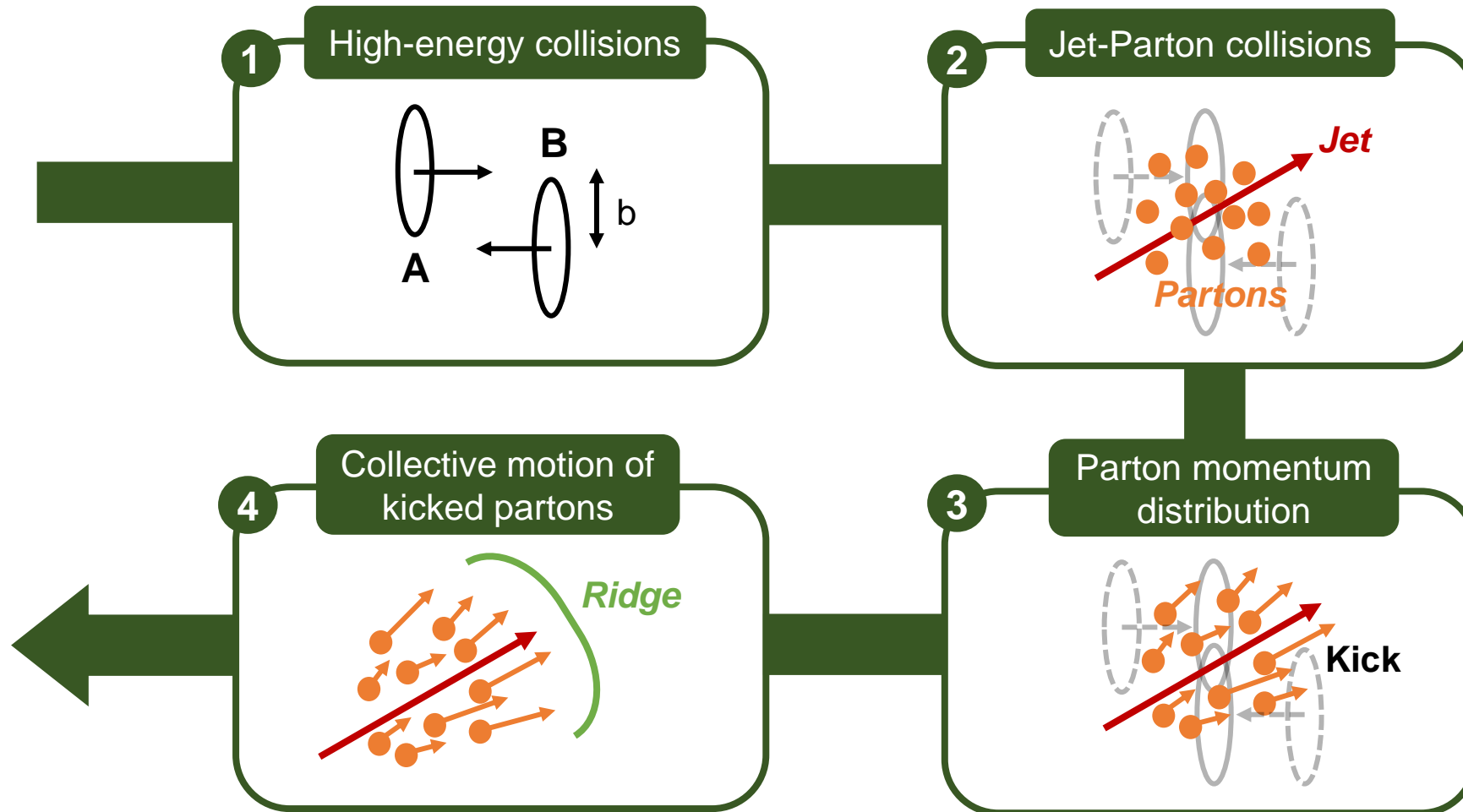
can explain the near-side long-range ridge structure in small systems.



Momentum Kick Model

How explain the ridge structure?

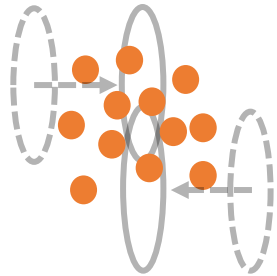
Kinematic process



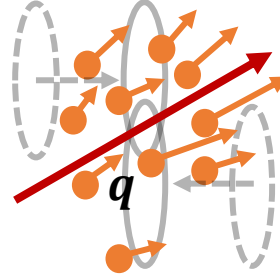
Formalism

for the MKM

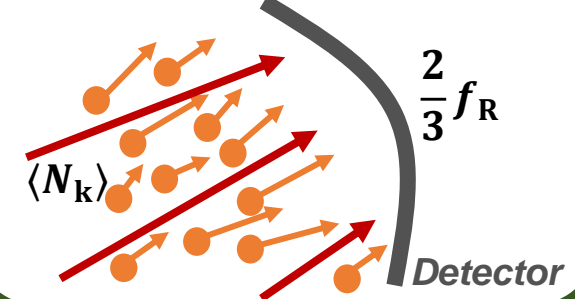
Initial parton momentum distribution



Final parton momentum distribution



Collective motion of kicked partons



$$\mathbf{P}_i(p_{T_i}, \Delta y_i, \Delta \phi_i)$$

→ parameterize

$$\mathbf{P}_f(p_{T_f}, \Delta \eta_f, \Delta \phi_f)$$

$$= [\mathbf{P}_i(p_{T_i}, \Delta y_i, \Delta \phi_i) \times L^*]_{\mathbf{p}_i = \mathbf{p}_f - \mathbf{q}^\dagger} \times J^\ddagger(\Delta y \rightarrow \Delta \eta)$$

* Lorentz invariant ensuring factor

† Average momentum transfer

‡ Jacobian

$$Y_{\text{assoc}}(p_{T_f}, \Delta \eta_f, \Delta \phi_f)$$

$$= \frac{2}{3} \times f_R^* \times \langle N_k \rangle^\dagger \times \mathbf{P}_f(p_{T_f}, \Delta \eta_f, \Delta \phi_f)$$

* Survival factor reaching the detector

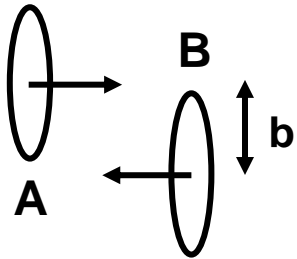
† The average number of kicked partons

※ q , f_R , and $\langle N_k \rangle$ are important parameters in this topic.

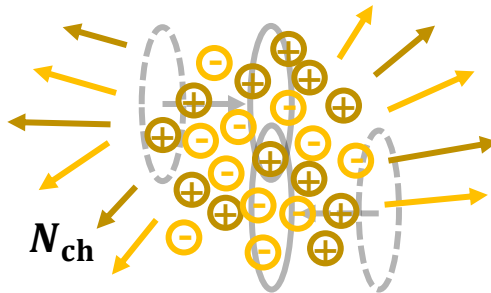
Formalism

for the multiplicity dependence

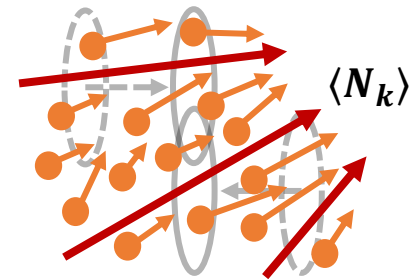
Glauber model



Multiplicity



The average number of kicked partons



$$\frac{dN_{\text{particip}}}{db'} = T_A^\dagger(\mathbf{b}_A) + T_B(\mathbf{b}_B)$$

† Thickness function.

$$N_{\text{ch}}(\mathbf{b}) = \frac{2}{3} \times \frac{\langle N_{\text{ch}} \rangle}{\langle N_{\text{particip}} \rangle} \times \int d\mathbf{b}' \frac{dN_{\text{particip}}}{db'}$$

$$\langle N_k \rangle(\mathbf{b}) = \int d\mathbf{b}' \frac{dN_{\text{particip}}}{db'} \times P_{\text{jet}}^* \times f_{\text{att}}^\dagger \times \sigma_{\text{jp}}^\ddagger \Big|_{\text{average}}$$

* Jet production probability.

† Jet attenuation factor.

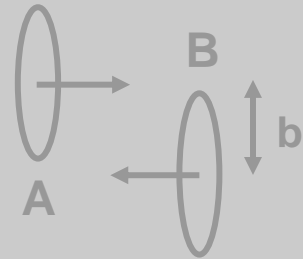
‡ Jet-Parton cross-section.

Formalism

for the multiplicity dependence

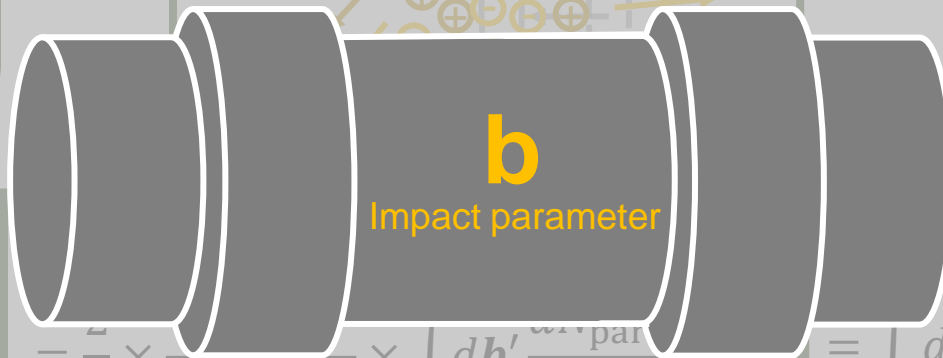
The impact parameter plays a role of a pipeline between N_{ch} and $\langle N_k \rangle$.

G



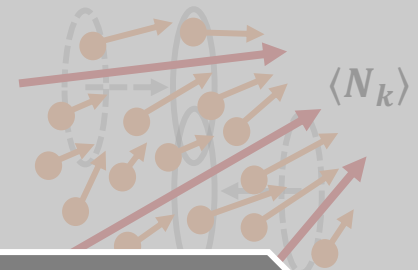
$$\frac{dN_{particp}}{db'} = T_{A \otimes A' \otimes B \otimes B'}$$

† Thickness function.



$$= \frac{4}{3} \times \frac{1}{\langle N_{particp} \rangle} \times \int db' \frac{dN_{particp}}{db'}$$

Number of kicked partons



$$= \int db' \frac{dN_{particp}}{db'} \times P_{jet}^* \times f_{att}^\dagger \times \sigma_{jp}^\ddagger \Big|_{average}$$

* Jet production probability.

† Jet attenuation factor.

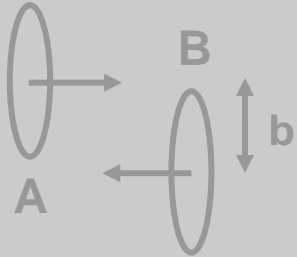
‡ Jet-Parton cross-section.

Formalism

for the multiplicity dependence

The matching result between N_{ch} and $\langle N_k \rangle$.

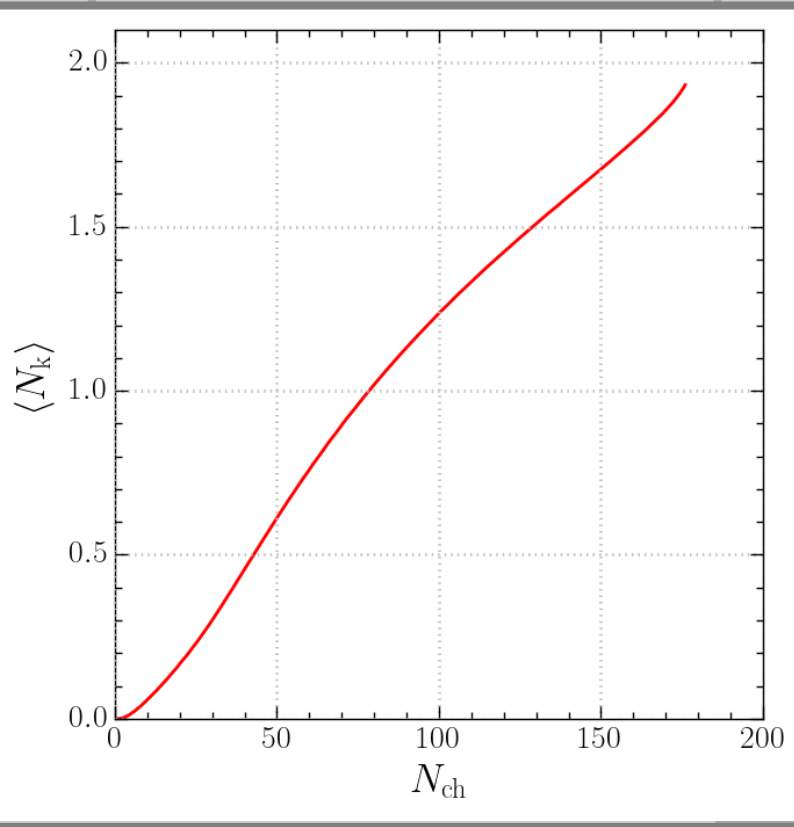
Glauber model



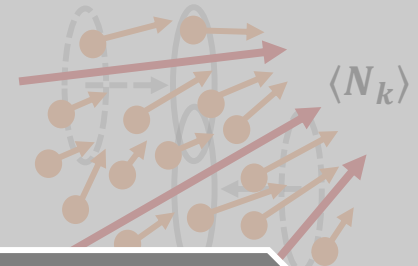
N_{ch}

$$\frac{dN_{particip}}{db'} = T_{A \otimes A} + T_{B \otimes B}$$

†Thickness function.



The average number of kicked partons



$\langle N_k \rangle$

$$db' \frac{dN_{particip}}{db'} \times P_{jet}^* \times f_{att}^\dagger \times \sigma_{jp}^\ddagger \Big|_{average}$$

† production probability.

‡ attenuation factor.

‡ Parton cross-section.

Application results

CMS data at $\sqrt{s} = 13$ TeV for pp collisions

Red circles → CMS data.

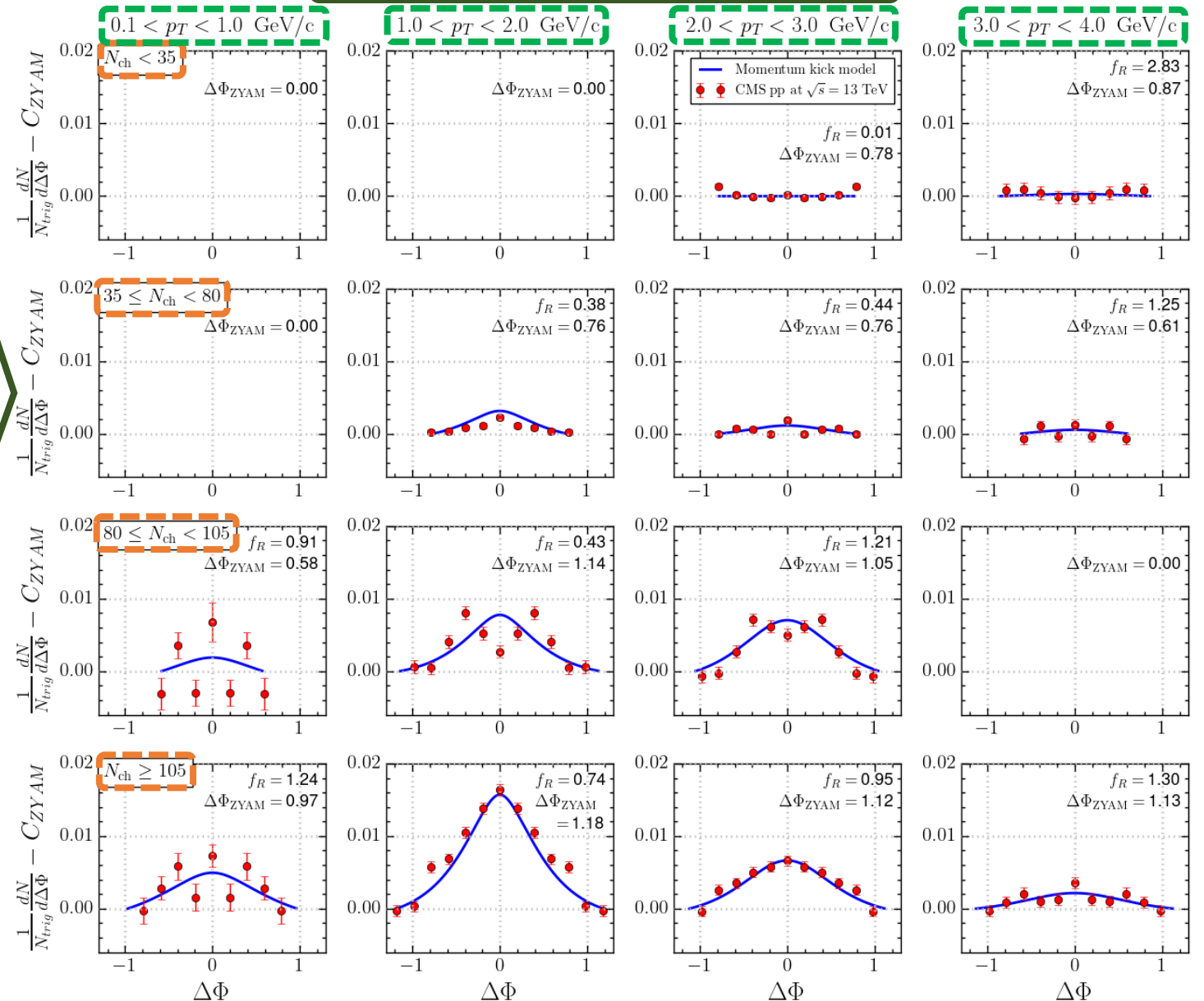
Blue curves → MKM results.

Columns → Different p_T ranges.

Rows → Different N_{ch} ranges.

- Averaged over $2 < |\Delta\eta| < 4$.
- ZYAM(zero-yield-at-minimum) procedure.
 - Minimum yield at $\Delta\phi_{ZYAM}$.
 - Making yield at $\Delta\phi_{ZYAM}$ zero by subtracting C_{ZYAM} .
- Least-Square-Fitting-Method: q and f_R .
 - $q = 1.2$ GeV/c.
 - f_R increases with p_T .

Yield per trigger as a function of $\Delta\Phi$

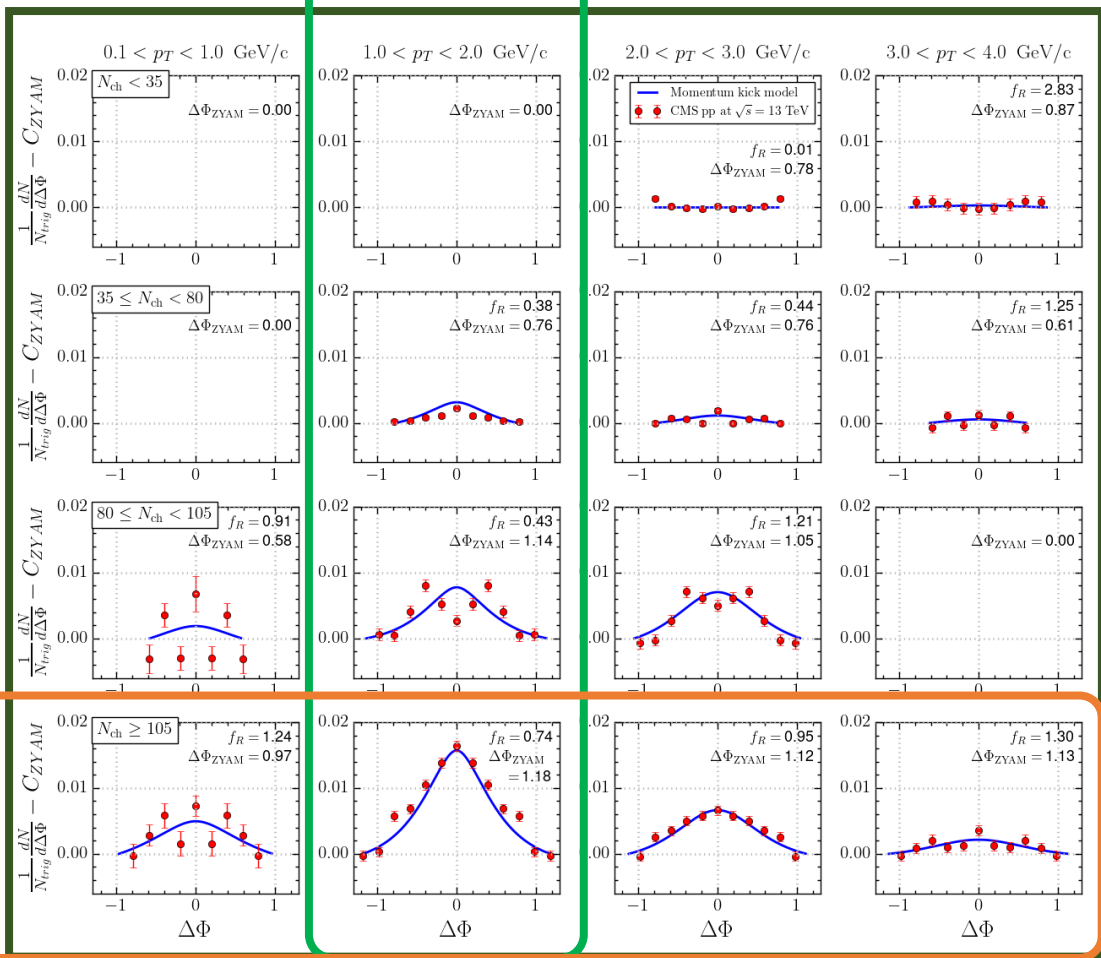


Application results

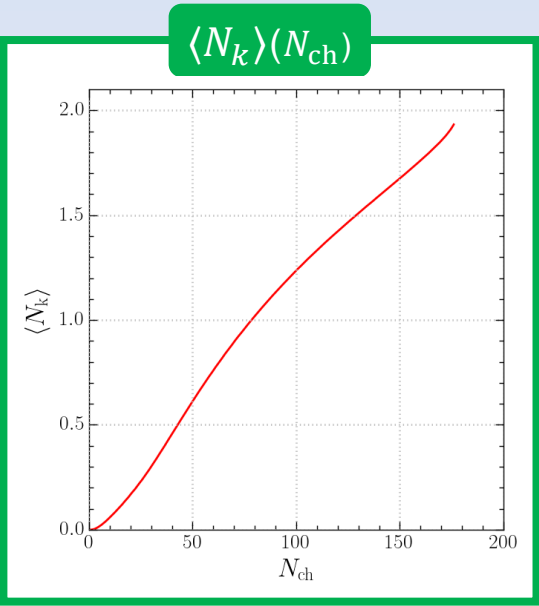
CMS data at $\sqrt{s} = 13$ TeV for pp collisions

$1.0 < p_T < 2.0$ GeV/c

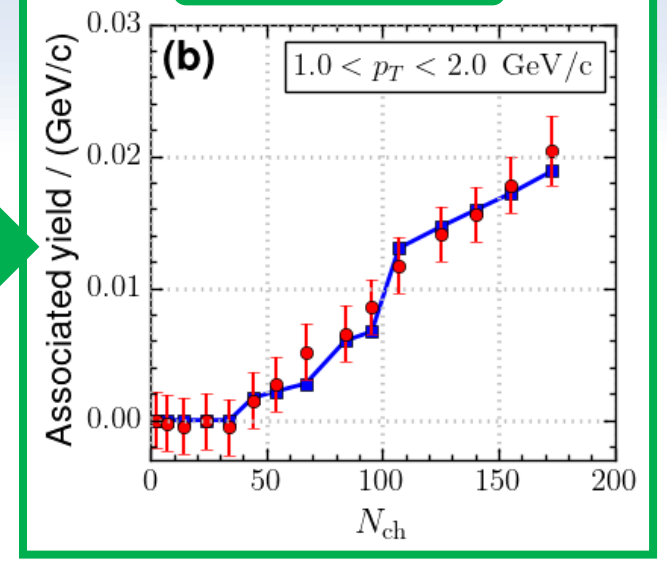
Integrated over $|\Delta\phi| < \Delta\phi_{ZYAM}$



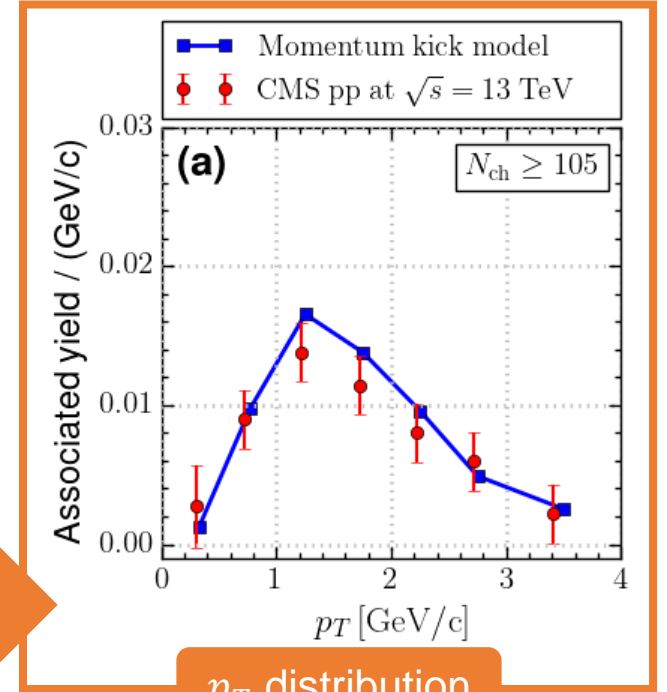
$N_{ch} \geq 105$



N_{ch} distribution



Integrated over $|\Delta\phi| < \Delta\phi_{ZYAM}$



p_T distribution

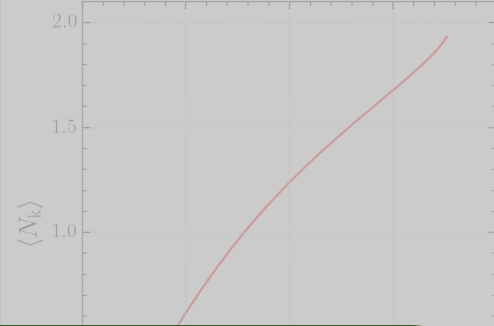
Application results

CMS data at $\sqrt{s} = 13$ TeV for pp collisions

$1.0 < p_T < 2.0$ GeV/c

Integrated over $|\Delta\phi| < \Delta\phi_{ZYAM}$

$\langle N_k \rangle (N_{ch})$



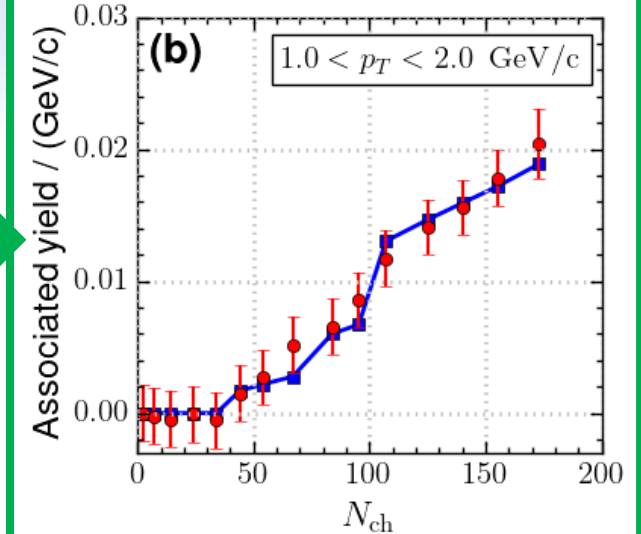
CMS Collaboration raised two questions

- Q1) "Ridge yield shows a linear increase with N_{ch} ."
- Q2) "Ridge yield reaches a maximum around $p_T \approx 1$ GeV/c."

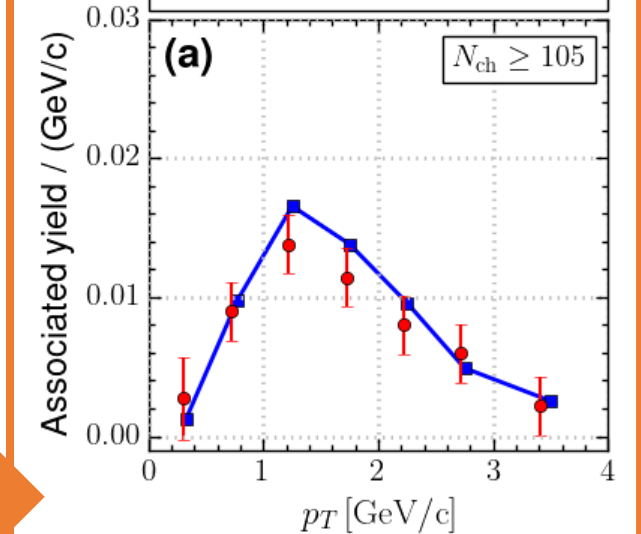
MKM can give a theoretical basis for these questions

- A1) This linearity is attributed to $\langle N_k \rangle$.
- A2) $q = 1.2$ GeV/c: The average momentum transfer is active at $p_T = 1.2$ GeV/c.

N_{ch} distribution

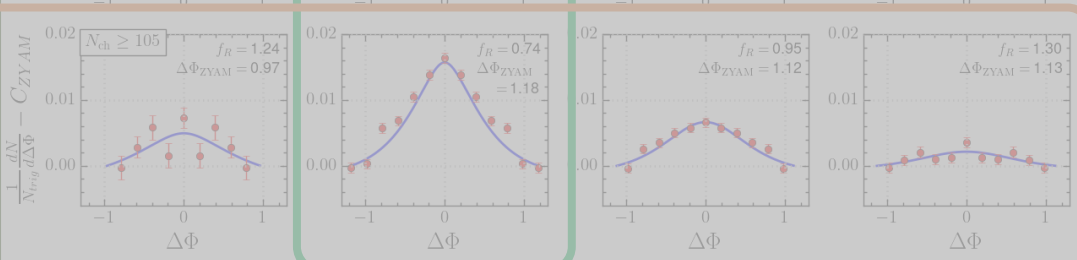


Legend:
■ Momentum kick model
● CMS pp at $\sqrt{s} = 13$ TeV



p_T distribution

$N_{ch} \ge 105$



Integrated over $|\Delta\phi| < \Delta\phi_{ZYAM}$

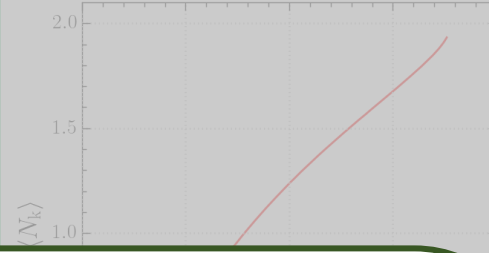
Application results

CMS data at $\sqrt{s} = 13$ TeV for pp collisions

$1.0 < p_T < 2.0$ GeV/c

Integrated over $|\Delta\phi| < \Delta\phi_{ZYAM}$

$\langle N_k \rangle(N_{ch})$



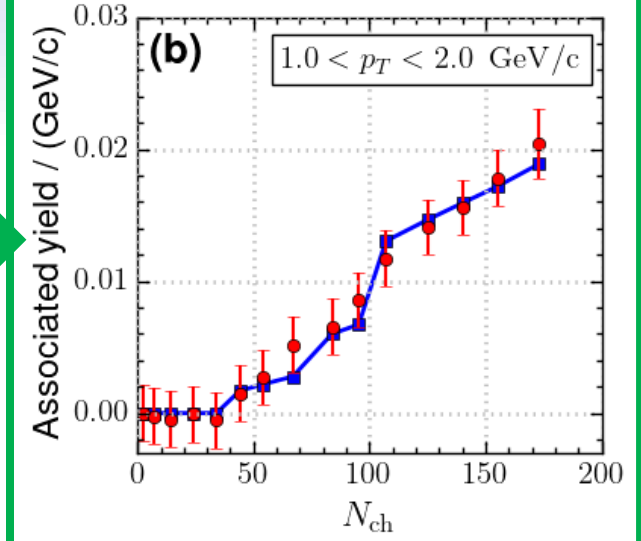
CMS Collaboration

- Near-side long-range ridge structures: at $\sqrt{s} = 13$ TeV **vs** at $\sqrt{s} = 7$ TeV.
 - The ridge structures for pp collisions do not have clear collision energy dependence.

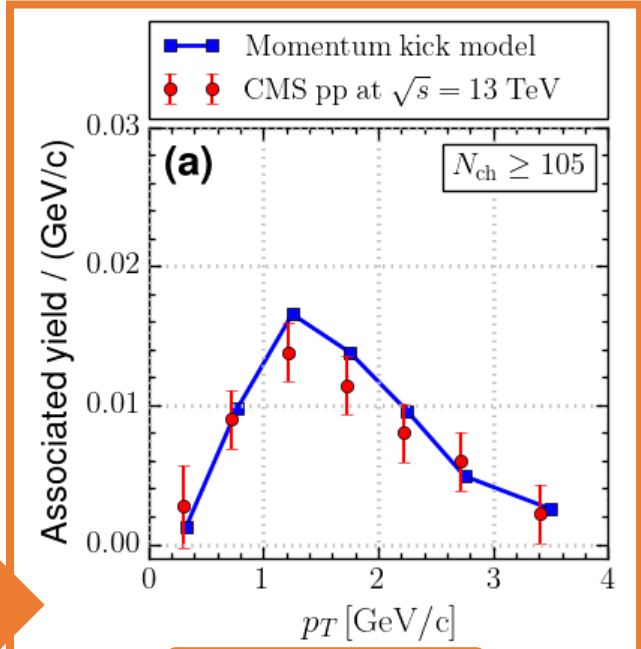
MKM predictions

- Around $q = 1.2$ GeV/c, regardless of collision energy for pp collisions.
 - Confirming $q = 1.1$ GeV/c at $\sqrt{s} = 7$ TeV.
- LHC Run3 is conducting measurements for pp collisions at $\sqrt{s} = 5.3$ & 8.5 TeV
 - We can try!

N_{ch} distribution

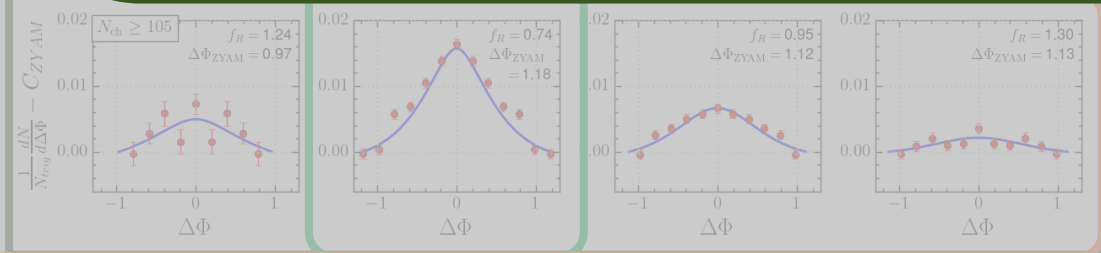


Legend: Momentum kick model (blue squares), CMS pp at $\sqrt{s} = 13$ TeV (red circles)



p_T distribution

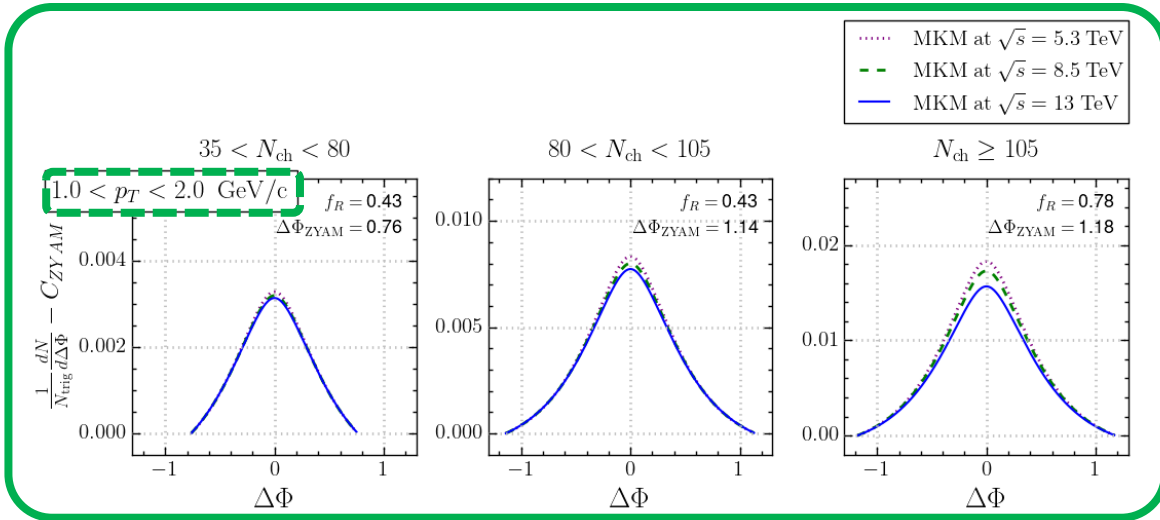
$N_{ch} \ge 105$



Integrated over $|\Delta\phi| < \Delta\phi_{ZYAM}$

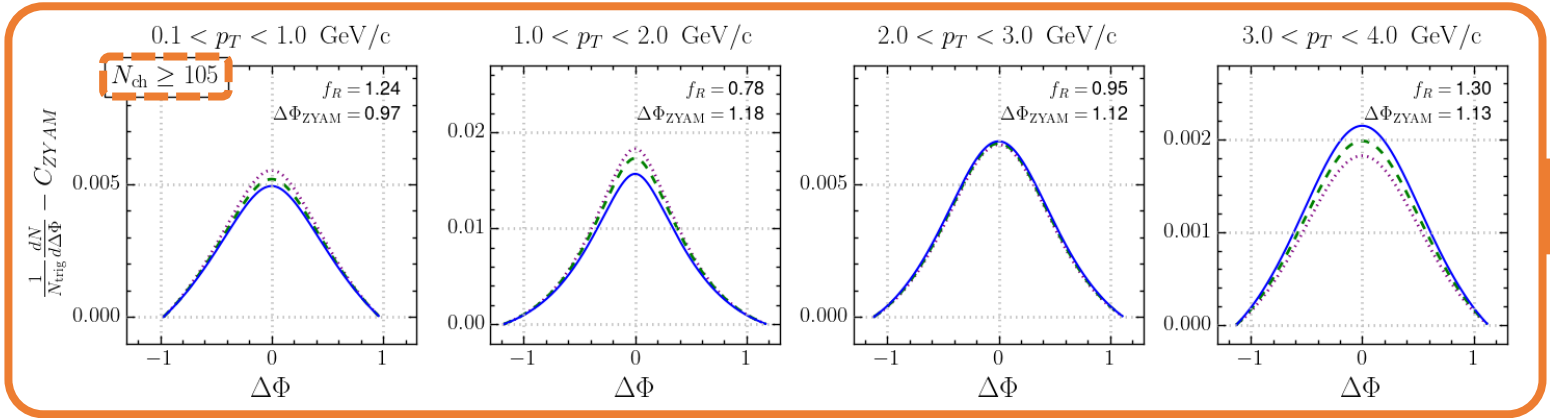
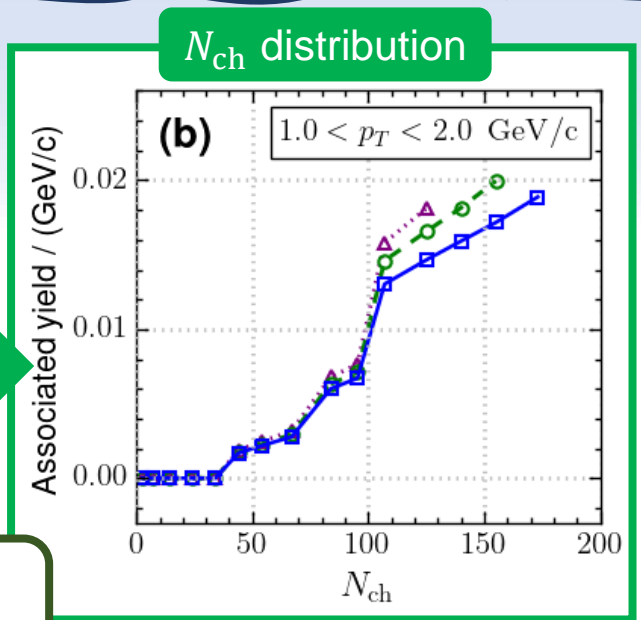
Predictions

at $\sqrt{s} = 5.3$ and 8.5 TeV for pp collisions

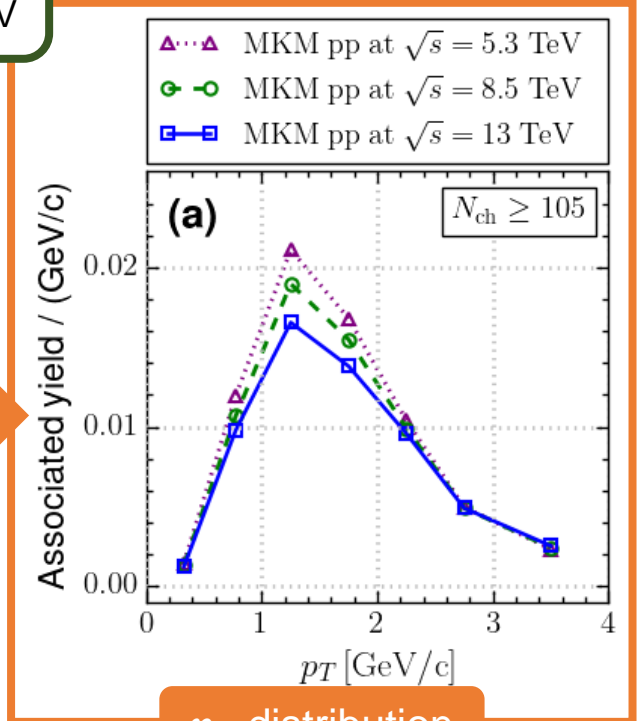


Integrated over $|\Delta\phi| < \Delta\phi_{ZYAM}$

- $q = 1.2$ GeV
- Using f_R & $\Delta\Phi_{ZYAM}$ at $\sqrt{s} = 13$ TeV



Integrated over $|\Delta\phi| < \Delta\phi_{ZYAM}$



p_T distribution

Summary

- MKM explains the near-side long-range ridge structure in small systems.
- By linking $\langle N_k \rangle$ with N_{ch} via impact parameter, MKM has multiplicity dependence.
- MKM with multiplicity dependence successfully describes the CMS data at $\sqrt{s} = 13$ TeV.
- CMS Collaboration provided a good surmise that ridge structures for pp collisions do not have clear collision energy dependence.
- Through the result of $q = 1.2$ GeV/c, MKM can predict the ridge structures at $\sqrt{s} = 5.3$ & 8.5 TeV.

Slide 2

Motivation

Ridge structure

- Two-particle(trigger and associated particles) correlation ph
- Similar to "mountain ridge."
- Provide insight into particle production.

Heavy-Ion collisions (such as PbPb and AuAu collisions) → Explained well by QGP (hydrodynamic models) → Sr

Insufficient density and temperature

Therefore, the hydrodynamic

∴ **Momentum Kick Model** can explain the near-side long

Slide 3

Momentum Kick Model

How explain the ridge structure?

Kinematic process

- High-energy collisions
- Jet-Parton collisions
- Parton momentum distribution
- Collective motion of kicked partons

Slide 4

Formalism for the MKM

Initial parton momentum distribution → parameterize

Final parton momentum distribution

$P_f(p_T, \Delta\eta, \Delta\phi) = [P_i(p_T, \Delta\eta, \Delta\phi) \times L]_{p_T=p_T-q} \times f^{\text{surv}}(\Delta y \rightarrow \Delta\eta)$

∴ q , f_R , and $\langle N_k \rangle$ are important parameters in this topic

Slide 5

Formalism for the multiplicity dependence

Glauber model → Multiplicity

$N_{ch}(b) = \frac{2}{3} \times \frac{\langle N_{ch} \rangle}{\langle N_{partic} \rangle} \times \int db' dN_{partic} \frac{dN_{partic}}{db'}$

$\langle N_k \rangle(b) = \int db' \frac{dN_{partic}}{db'}$

Application results

CMS data at $\sqrt{s} = 13$ TeV for pp collisions

Red circles → CMS data. Blue curves → MKM results.

Columns → Different p_T ranges. Rows → Different N_{ch} ranges.

- Averaged over $2 < |\Delta\eta| < 4$.
- ZYAM(zero-yield-at-minimum) procedure.
 - Minimum yield at $\Delta\phi_{ZYAM}$
 - Making yield at $\Delta\phi_{ZYAM}$ zero by subtracting C_{ZYAM}
- Least-Square-Fitting-Method q and f_R .
 - $q = 1.2$ GeV/c.
 - f_R increases with p_T .

Slide 7

Application results

CMS data at $\sqrt{s} = 13$ TeV for pp collisions

1.0 < p_T < 2.0 GeV/c. Integrated over $|\Delta\eta| < \Delta\phi_{ZYAM}$

Slide 8

Application results

CMS data at $\sqrt{s} = 13$ TeV for pp collisions

CMS Collaboration raised two questions

Q1) "Ridge yield shows a linear increase with N_{ch} ."

Q2) "Ridge yield reaches a maximum around $p_T \approx 1$ GeV/c."

MKM can give a theoretical basis for these questions

A1) This linearity is attributed to $\langle N_k \rangle$.

A2) $q = 1.2$ GeV/c. The average momentum transfer is active at $p_T = 1.2$ GeV/c.

Slide 9

Application results

CMS data at $\sqrt{s} = 13$ TeV for pp collisions

CMS Collaboration

- Near-side long-range ridge structures: at $\sqrt{s} = 13$ TeV vs at $\sqrt{s} = 7$ TeV
- The ridge structures for pp collisions do not have clear collision energy dependence.

MKM predictions

- Around $q = 1.2$ GeV/c, regardless of collision energy for pp collisions.
- Confirming $q = 1.1$ GeV/c at $\sqrt{s} = 7$ TeV.
- LHC Run3 is conducting measurements for pp collisions at $\sqrt{s} = 5.3$ & 8.5 TeV
- We can try!

Slide 10

N_k Predictions

at $\sqrt{s} = 5.3$ and 8.5 TeV for pp collisions

Integrated over $|\Delta\eta| < \Delta\phi_{ZYAM}$

$q = 1.2$ GeV

Using f_R & $\Delta\phi_{ZYAM}$ at $\sqrt{s} = 13$ TeV

N_{ch} distribution

Integrated over $|\Delta\eta| < \Delta\phi_{ZYAM}$

p_T distribution

Thank you!
Please questions ☺

BACK UP

Formalism

● Associated Yield

$$\triangleright \left[\frac{1}{N_{\text{trig}}} \frac{dN_{\text{ch}}}{p_T dp_T d\Delta\eta d\Delta\phi} \right]_{\text{total}}^{AA} = \left[f_R \frac{2}{3} \langle N_k \rangle \frac{dF}{p_T dp_T d\Delta\eta d\Delta\phi} \right]_{\text{ridge}}^{AA} + \left[f_J \frac{dN_{\text{jet}}^{pp}}{p_T dp_T d\Delta\eta d\Delta\phi} \right]_{\text{jet}}^{AA}$$

● Ridge

$$\triangleright \frac{dF}{p_T dp_T d\eta d\phi} = \left[\frac{dF}{p_{Ti} dp_{Ti} dy_i d\phi_i} \frac{E}{E_i} \right]_{p_i=p-q} \times \sqrt{1 - \frac{m_\pi^2}{(m_\pi^2 + p_T^2) \cosh^2 y}}$$

$$\triangleright \frac{dF}{p_{Ti} dp_{Ti} dy_i d\phi_i} = A_{\text{ridge}} (1 - x)^a \frac{e^{-\sqrt{m_\pi^2 + p_{Ti}^2}/T}}{\sqrt{m_d^2 + p_{Ti}^2}}$$

$$\triangleright x = \frac{\sqrt{m_\pi^2 + p_{Ti}^2}}{m_b} e^{|y_i| - y_b}$$

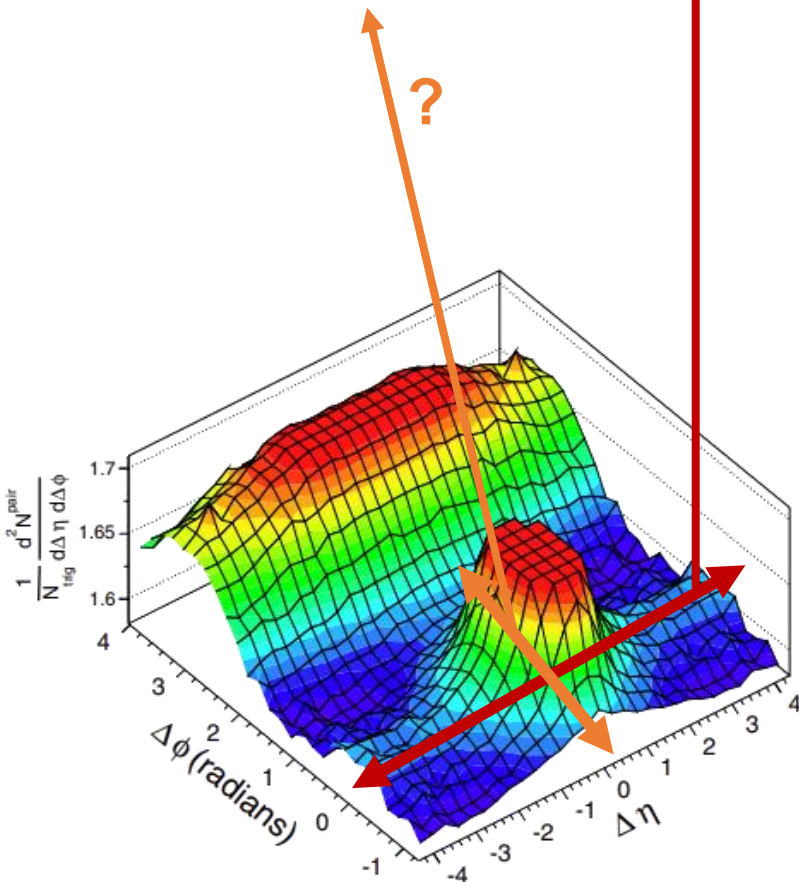
$$\triangleright y_b = \cosh^{-1} \left(\frac{\sqrt{S_{NN}}}{2m_b} \right)$$

● Jet

$$\triangleright \frac{dN_{\text{jet}}^{pp}}{p_T dp_T d\Delta\eta d\Delta\phi} = N_{\text{jet}} \frac{\exp \left[\left(m_\pi - \sqrt{m_\pi^2 + p_T^2} \right) / T_{\text{jet}} \right]}{T_{\text{jet}} (m_\pi + T_{\text{jet}})} \times \frac{1}{2\pi\sigma_\phi^2} e^{-[(\Delta\phi)^2 + (\Delta\eta)^2] / 2\sigma_\phi^2}$$

Question

- The ridge structure appears broadly in $\Delta\eta$.
- What about in $\Delta\phi$?

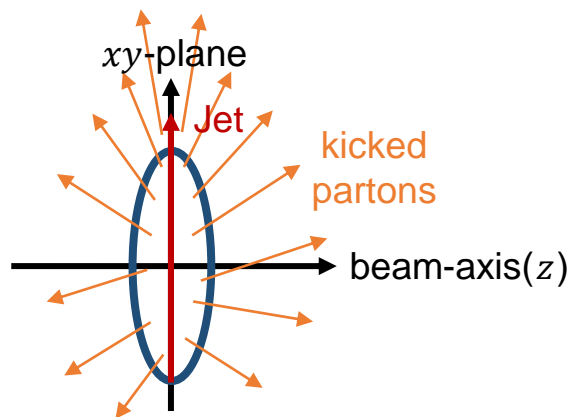


In the case of $\Delta\phi \approx 0$

- Pseudo-rapidity of two particles,

$$\Delta\eta = \eta_{\text{kp}} - \eta_{\text{jet}} = \frac{1}{2} \ln \frac{p_0 + p_3}{p_0 - p_3},$$

where $\eta_{\text{jet}} = 0$ for convenient calculation.



- Final parton momentum
- ✓ Assuming that $p_3 = 1.0$ GeV.

- 1) In the case of $p_0 = 1.1$ GeV,

$$\triangleright \Delta\eta = \frac{1}{2} \ln \frac{1.1+1.0}{1.1-1.0} = 1.5.$$

- 2) In the case of $p_0 = 1.01$ GeV,

$$\triangleright \Delta\eta = \frac{1}{2} \ln \frac{1.01+1.0}{1.01-1.0} = 2.7.$$

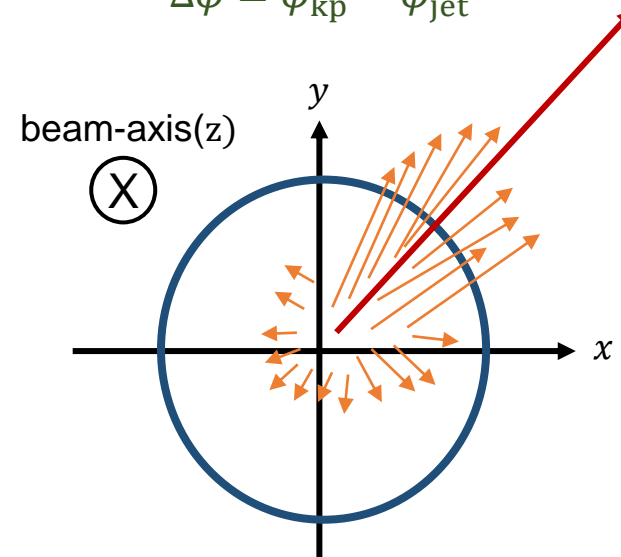
- 3) In the case of $p_0 = 1.001$ GeV,

$$\triangleright \Delta\eta = \frac{1}{2} \ln \frac{1.001+1.0}{1.001-1.0} = 3.8. \text{ etc...}$$

In the case of $\Delta\eta \approx 0$

- The region of $\Delta\phi \approx 0$ is relatively more dominant than the other regions.

$$\Delta\phi = \phi_{\text{kp}} - \phi_{\text{jet}}$$



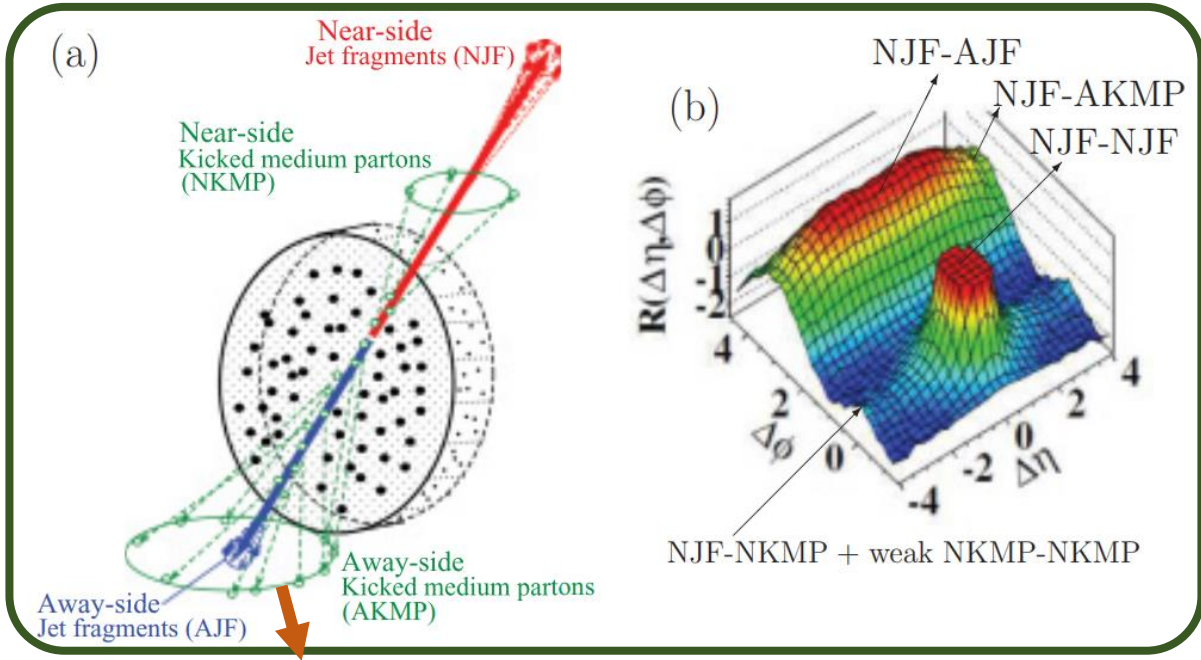
Conclusion

- In the case of $\Delta\phi \approx 0$, the ridge structure appears broadly in $\Delta\eta$.
- In the case of $\Delta\eta \approx 0$, the ridge structure is aligned to the direction of jet.

Momentum Kick Model

Other processes

PHYSICAL REVIEW C 84, 024901 (2011)



Two particle correlation
“trigger” + “associated” particles

Many different correlations

- ① NJF-NJF correlation
- ② NJF-NKMP correlation
- ③ NJF-AKMP correlation
- ④ NJF-AJF correlation
- ⑤ NKMP-NKMP correlation
- ⑥ NKMP-AKMP correlation
- ⑦ NKMP-AJF correlation

high- p_T trigger particles **NJF**

+

low- p_T trigger particles **NKMP**



Minimum- (p_T) -bias

The strength of the NJF-AJF correlation will be substantially quenched. Therefore, it will become a broad shape.

- Near-side** ($\Delta\phi \sim 0$): ①, ②, ⑤ → We focus on it!
- Away-side** ($\Delta\phi \sim \pi$): ③, ④, ⑥, ⑦